Structural Characterization of the 1-Butyl-3-methylimidazolium Chloride Ion Pair Using ab Initio Methods

Patricia A. Hunt* and Ian R. Gould

Chemistry Department, Imperial College London, London SW7 2AZ, United Kingdom

Received: August 24, 2005; In Final Form: November 3, 2005

Ⓦ **This paper contains enhanced objects available on the Internet at http://pubs.acs.org/jpcafh.**

Ab initio theoretical methods are used to investigate the gas-phase ion pairs of the ionic liquid 1-butyl-3-methylimidazolium chloride. Multiple stable conformers with the chloride anion positioned (in-plane) around the imidazolium ring or above the C^2-H bond are determined. The relative energy ordering of the conformers is examined at the B3LYP, MP2, and CCSD(T) levels. Zero-point energies, BSSE, and basis set effects are examined. For accurate results, correlation (dispersion) effects must be included. The most stable conformers are essentially degenerate and have the chloride H-bonding to, or lying above, the C^2-H bond. Other conformers are found to lie ∼30 and ∼60 kJ mol^{-1} higher in energy. Results are compared with those from recent simulations and experimental studies. The effect of the chloride anion on rotation of the butyl chain is investigated and found to lower some rotational barriers while enhancing others. The origin of the rotational barriers is determined. The number and type of hydrogen bonds formed between the imidazolium cation and chloride anion is found to vary significantly among conformers. No evidence of a possible intra $C^{alkyl}-H\cdots\pi$ interaction is obtained; however, hints of a $Cl\cdots\pi$ interaction are found. The vibrational spectrum of each conformer is examined, and the origin of multiple (H-bonding) features in the vibrational spectrum of the ionic liquid explained.

Introduction

Recently, room-temperature ionic liquids (IL) have elicited substantial interest both in academia and in industry.[1−7] Ionic liquids are typically composed of organic cations (for example, 1-butyl-3-methylimidazolium, Scheme 1) and inorganic anions (for example, chloride, Cl^-). A promising feature of ILs is the ability to tailor physicochemical properties via selecting an appropriate ion pair. However, at present, there is no way of determining a priori which particular pairing will produce the desired properties. The ability to predict the physicochemical properties of an unknown ionic liquid will depend (in part) on understanding the molecular-level interactions. To obtain a deeper understanding of the fundamental molecular-level interactions occurring in a prototypical ionic liquid, we have undertaken an analysis of the gas-phase 1-butyl-3-methylimidazolium chloride ion pair. In this article, we adopt a $[C_nC_m\text{im}]$ notation (where *n* and *m* denote the length of the alkyl groups on N^1 and N^3, respectively) for naming the imidazolium cations.[5] For example, $[C_4C_1\text{im}]^+$ denotes 1-butyl-2-methyl-imidazolium. The aim of the present work is to study, using ab initio quantum chemical methods, the structure and H-bonding in an ion pair from the room-temperature ionic liquid $[C_4C_1\text{im}]Cl$. One intention is to provide an ab initio reference for comparison with classical and semiclassical MD computations. In addition, the applicability and reliability of ab initio methods at various levels of theory and basis set sophistication is explored.

Ionic species such as NaCl are solid at room temperature and melt at elevated temperatures, forming molten salts. ILs, however, tend to be liquid at room temperatures. The low melting point of ILs has been rationalized: asymmetrical and charge-diffuse cations frustrate local packing, and repulsive forces between the charge-neutral organic substituents and highly ionic components make tight packing difficult.[1,8] However, the situation is more complicated than this intuitive explanation implies.[3,8] Ionic liquids also exhibit a negligible vapor pressure and decompose before they vaporize; substantial attractive forces between the oppositely charged ions are assumed to restrict the release of single ions or ion pairs. Crystallographic,[9−13] spectroscopic,[14,15] neutron diffraction,[16,17] and classical molecular dynamics (MD) simulation[8,18,19] techniques also indicate that an extended 3D network of attractive H-bonds exist in many (but not all)[20] ILs. Thus, the interactions in an ionic liquid are very strong (as it is difficult for ions to escape into the vapor phase) and at the same time extremely disruptive (as the formation of a solid is hampered).

SCHEME 1: 1-Butyl-3-methylimidazolium Cation, $[C_4C_1\text{Im}]^+$

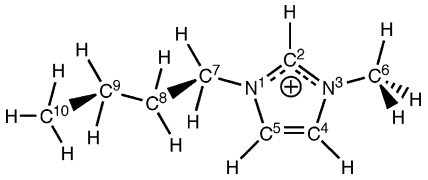

The ion pair is of intrinsic interest as a gas-phase species produced after decomposition and as a (possible) molecular unit within the ionic liquid. There is evidence from experimental[3,21,22] and simulation[8,23−27] studies that ions may diffuse through the solution together. However, there have also been suggestions that larger clusters form and may be important in both the liquid[28,29] and gas phases;[30] moreover, it has not been established

* p.hunt@imperial.ac.uk.

10.1021/jp0547865 CCC: $33.50
Published on Web 01/25/2006

that charge transport occurs via the movement of associated ion pairs.[3] By comparing the results of ab initio calculations with experimental liquid and solid-state structures, the effects due to interactions within an isolated ion pair can be distinguished from those that are dependent on the complex condensed-phase forces. Furthermore, if a relationship can be found between the gas-phase structures and the condensed-phase structures, ab initio computational studies of simple ion pairs can be used to understand and predict (through examination of the electronic structure and available structural configurations) selected features of ionic liquids. This would be advantageous, as calculations of this type are less demanding than large-scale classical simulations and thus could be used to guide the choice of an appropriate pairing before significant investment is made in synthesis and physical characterization.

The local structure of imidazolium ILs in the liquid and gas phases is not known in detail. Recent experimental[13,16,17,31] and computational[18,19,32,33] studies of the liquid phase agree that C^2—H···anion interactions dominate in the $C_nC_1$im halide-based ILs. However, they do not agree on the most likely position of the anion relative to C^2—H. Does the anion sit above the C^2, or does it interact primarily with the hydrogen atom? Recent (experimental and computational) studies suggest both possibilities, and thus, the local structures of these ILs are still under investigation. Neutron diffraction studies indicate that the position of the anion depends on the size of the anion: Cl anions prefer to remain in a ring around the H atom, with a lesser preference for lying above and below the center of the imidazolium ring.[16,17] However, in classical simulations, the anion tends to interact along the length of the C^2—H bond, preferring to remain above or below the plane containing the imidazolium ring. The fine details of the C^2—H···anion interaction also appear to be force field dependent.[18,19,33,34] Crystallographic studies indicate that the anion remains in-plane with the imidazolium ring interacting axially with the H-atom.[13,31] Car−Parrinello studies on the liquid phase suggest that the anions prefer to remain near the H-atom and show little evidence of an interaction above or below the plane of the imidazolium ring.[32,34] However, for a single ion pair in the gas phase, a position above or below the C^2 atom is preferred.[32] The anion can also be located close to the C^4—H and C^5—H units at the rear of the imidazolium ring. It has been noted that the spatial distributions of these carbon atoms with the chloride ion are sensitive to the intermolecular forces in a simulation, and the distributions obtained from ab initio MD differ from those obtained experimentally or via classical simulation.[32] For example, the relative probability of finding the Cl^- anion between the C^4—H and C^5—H units was found variously to be substaintial,[18] minimal,[33] and absent.[32] Del Popolo et al. have recently suggested that there is a directionality in the H···anion interaction of quantum mechanical origin, which classical point charge models have not yet reproduced.[32] The local structure of imidazolium ILs in the liquid and gas phases is clearly not well-established. In this investigation, the relative stability of gas-phase conformers is established and quantified at a quantum mechanical level.

The computational modeling of ionic liquids has primarily involved the use of classical simulation methodologies; classical molecular dynamics (MD) and Monte Carlo[35] methods have been used to investigate, primarily, the neat imidazolium-based ionic liquids (and particularly $[C_4C_1\text{im}][PF_6]$).[8,18,19,23,24,27,33,36−41] The success of a molecular simulation can depend critically on the quality of the model potential used.[33,37] However, the fitting of potentials to experimental data has not been possible for ionic liquids, and potentials have necessarily been postvalidated (using properties such as liquid densities and solid-state cell parameters).[18,19,25,33,35,37,38,41] High-level ab initio results can be used as a means of validation. Chaumont and Wipff, for example, have used ab initio binding energies to endorse an AMBER[42] based force field.[43−49] The inability of a classical model to reproduce features observed in gas-phase structures can indicate either the existence of structures primarily due to condensed-phase interactions or a deficiency in the classical potential. In the absence of good experimental data, a coincidence with ab initio determined behavior (such as predicting the same stable ion pair configurations) will support the accuracy of a good force field.

Many force fields are derived in part from ab initio computations. Components, such as partial charges, structures, and torsional parameters, are based on crystal structures[18] or ab initio optimizations carried out at relatively low levels of theory (HF and B3LYP),[33,35,37,38,41] although in some cases, the partial charges have been determined at higher levels of theory (MP2).[18,19,25,41] The imidazolium cation is aromatic and contains alkyl chains, both of which contribute significantly, via dispersion and van der Waals forces, to nonbonded interactions within the ionic liquid. The relative magnitude of the errors (both structural and energetic) introduced by low-level calculations needs to be established. The use of effective potentials in classical simulation should account for this neglect of correlation, and the effectiveness of potentials in recovering these contributions can be more firmly established by comparison with calculations that include a significant amount of correlation. Our computations suggest that the relative stability of different anion positions around the cation is highly dependent on the nonbonding and diffusive interactions. Moreover, an indication of the errors introduced through the neglect of dispersion for density functional theory (DFT)-based ab initio molecular dynamics can be obtained. A number of calculations of this type have recently been published.[32,34]

There are still relatively few ab initio quantum chemical calculations on the gas-phase ion pairs that make up ionic liquids.[30,46,50−53] Early studies are limited to the chloroaluminate ILs.[54−56] Some studies include only the imidazolium cations and have primarily been aimed at producing parameters for force field methods.[23,33,41,57] Turner et al. have attempted a systematic analysis of small $[C_nC_1\text{im}]$ cations ($n = 1$, 2, and 4) with the series of halides spanning F through I.[58] Lopes et al. have examined the potential energy surface for rotation of the alkyl groups and obtained more than one minima.[41]

This paper is organized as follows: Computational methods and technical details are described in the computational details section. Results are presented, and then, we go on to discuss specific aspects in more detail. Possible conformational arrangements for the chloride anion around the cation are considered. The extent of H-bonding in the ion pair complexes is investigated, both from a structural perspective and through examination of the vibrational (IR) spectrum. The effects of rotation in the butyl chain both with and without a chloride anion present are explored. The ability of lower-level methods and basis sets to qualitatively reproduce the rotational potential energy surface is examined. Initial studies reveal that several of the lowest-energy conformers are almost degenerate; we examine these at higher levels of theory and consider both basis set superposition effects (BSSE) and zero-point energy (ZPE) corrections. Throughout, our results are compared to crystal structure and neutron diffraction experiments, as well as previously reported ab initio, Car−Parrinello MD, and classical

MD studies. In the final section, we summarize our most important conclusions.

Computational Details

HF, DFT, and MP2 (frozen core)-level calculations using 3-21G,[59,60] 3-21G(d),[61] and 6-31++G(d,p)[62−64] basis sets have been carried out with the *Gaussian 03* suite of programs.[65] DFT calculations primarily use the B3LYP (Becke's three-parameter exchange functional[66] in combination with the Lee, Yang, and Parr correlation functional[67]); however, in certain cases, the PBE1PBE (1997 hybrid functional of Perdew, Burke, and Ernzerhof[68]) was employed. The generalized gradient corrected functionals used here are unable to fully recover dispersion effects.[69] In an effort to estimate the amount of neglected dispersion, selected structures were examined at higher levels of theory, principally MP2/6-31++G(d,p); however, selected structures have also been examined at the CCSD(T) level using cc-pVDZ and aug-cc-pVDZ[70,71] basis sets and the *MOLCAS* suite of programs.[72] Because of the substantial computational cost of these calculations, they are single-point energies computed at optimized MP2/6-31++G(d,p) geometries. It has been suggested that the dispersion forces are more significant than BSSE,[51] and we have attempted to quantify this; the BSSEs have been determined for a selection of structures.

From the crystal structure and previous MD studies, it is known that a number of anions surround each cation (and vice versa). Initial ion pair structures were determined by placing the Cl anion around the cation in "chemically intuitive" positions where interaction with hydrogen atoms of the cation was a possibility. Structures were preoptimized to a local minimum using one of the following: HF/3-21G, HF/6-31G, or B3LYP/3-21G(d). Each unique structure was then further optimized, under no symmetry constraints, at the B3LYP/6-31++G(d,p) level of theory. No stable structure with the Cl sitting above the imidazolium could be located at the HF/3-21G level of theory; thus, this conformer was directly optimized at the higher level of theory using as a starting point the optimized coordinates of $[C_2C_1im]Cl$, kindly supplied by M. Pópolo.[32]

Fully optimizing many of the structures was made difficult by a very flat potential energy surface; convergence criteria were tightened from the Gaussian defaults to 10^{-9} on the density matrix and 10^{-7} on the energy matrix. In isolated cases, optimization was terminated on the basis of negligible forces (root-mean-square (rms) < 0.000 004; maximum force < 0.000 025); in each case, the lowest vibrational modes were examined, and the lowest (i.e., the 6 modes subtracted because of translational and rotational motion of the center of mass of the molecule) had a magnitude less than 7 cm^{-1}. For calculations at the B3LYP level, the numerical integration grid was improved from the default; a pruned (optimized) grid of 99 radial shells and 590 angular points per shell was requested. The enhanced criteria were maintained when performing single-point calculations (for example, frequency and counterpoise corrections). Vibrational frequencies and the zero-point vibrational energy correction (ΔZPE) have been obtained within the harmonic approximation for each monomer and ion pair at the B3LYP level. Basis set superposition errors (ΔBSSE) have been determined using the counterpoise method.[51]

Results

The $[C_4C_1im]Cl$ ion pair structures obtained can be classified according to the primary cation−anion interactions, Figure 1. There are four associations in which the chloride remains roughly in-plane with the imidazolium ring and one in which the chloride lies above the plane of imidazolium ring, and more specifically above the C_2−H bond. A symmetry-related structure with the Cl anion below (rather than above) the ring also exists. C^2 can be seen as having four different substituents (counting the anion), and thus, these structures are "chiral"; in each case, we have investigated only one of the two configurations. Thus, six conformers have been determined, consistent with MD findings.[16] These conformers will be identified as "front" (interaction through C^2−H), "top" (chloride above the imidazolium ring), "butside" (positioned between N^1 and C^5), "methside" (positioned between N^3 and C^4), and "back" (positioned between C^4 and C^5). These sites can be linked to the density maps produced from molecular dynamics simulations.[18,19,33] The computed front, butside, methside, and back structures have been found in the crystal structures of $[C_4C_1im]Cl$; the top conformer has not been observed in these crystal structures. Our attempts to optimize ion pairings where the Cl anion is associated primarily with the alkyl chain (identified from crystal structure) were unsuccessful, indicating that, in this case, primary stabilization is from other interactions formed at the same time (such as those already identified).

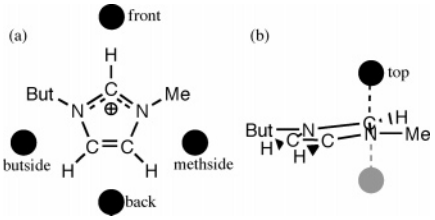

Figure 1. Location of primary cation−anion interaction sites for $[C_4C_1im]Cl$: (a) Cl anion in-plane, (b) Cl anion out-of-plane.

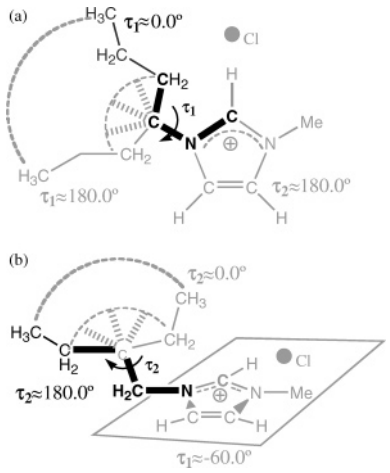

Figure 2. Description of the torsion angles, $\tau_1 = C^2—N^1—C^7—C^8$ and $\tau_2 = N^1—C^7—C^8—C^9$.

After the "gross" position of the anion is determined, a number of subconfigurations are possible because of variation in the orientation of alkyl groups. The most stable orientation of the methyl group involves one C^6—H in-plane with C^2—H, except where the anion is positioned behind the methyl group or is in the top position. Alkyl motion beyond the N^1—C^7 bond is facile, and multiple orientations of the butyl chain are possible.[19,31,58] Three key conformers were determined with respect to the butyl chain orientation; these are defined by the torsion angles: $\tau_1 = C^2—N^2—C^7—C^8$ and $\tau_2 = N^2—C^7—C^8—C^9$ (Figure 2). Structures with the anion in a similar position but the butyl chain rotated are identified by adding a ($\tau_2 \approx 180°$), b ($\tau_2 \approx 60°$), and c ($\tau_2 \approx -60°$), to the primary position designator. τ_1 determines the orientation of the butyl chain with respect to the planar imidazolium ring, while τ_2 reflects internal

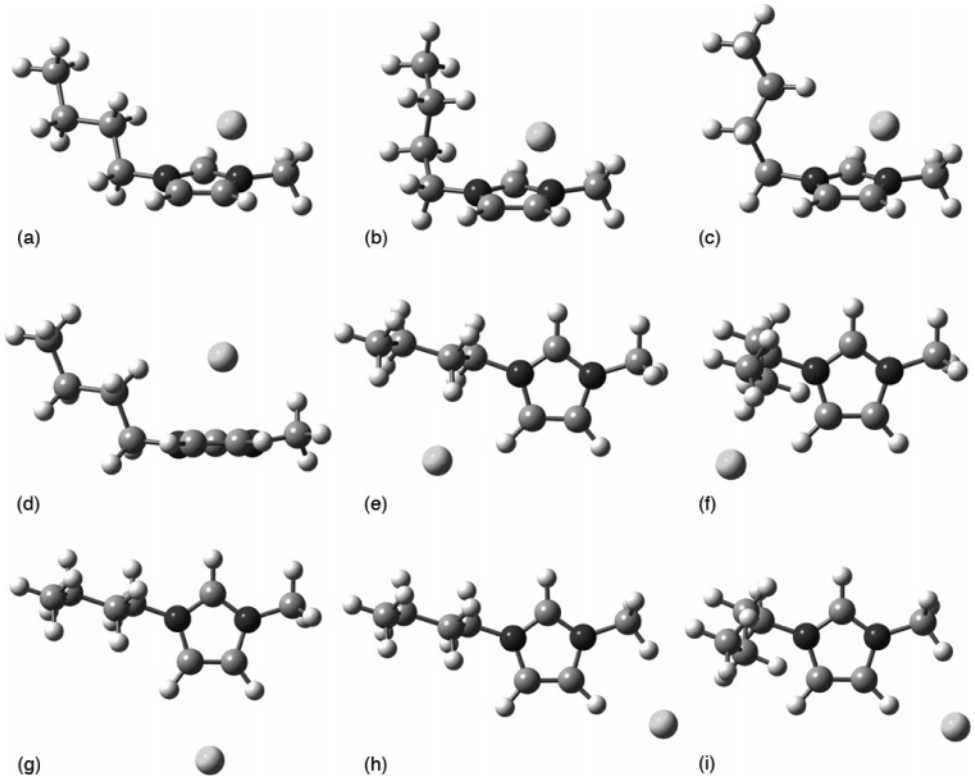

Figure 3. Stable [C_4C_1im]Cl structures: (a) front-1a, (b) front-1b, (c) front-1c, (d) top-2, (e) butside-3a, (f) butside-3b, (g) back-5a, (h) methside-4a, and (i) methside-4b.

Ⓦ 3D rotatable images of Ⓦ front-1a, Ⓦ front-1b, and Ⓦ front-1c in xyz format are available.

TABLE 1: Ring Bond Distances for the Crystalline [C_4C_1im]Cl and the Gas-Phase Conformers (in Å)[a]

	X-ray ortho[31]	X-ray mono[31]	X-ray mono[13]	MP2 front-1b	B3LYP front-1b	B3LYP top-2	B3LYP butside-3b	B3LYP methside-4b	B3LYP back-5a
N^1-C^2	1.322	1.331	1.325	1.344	1.341	1.341	1.337	1.343	1.342
C^2-N^3	1.337	1.329	1.324	1.344	1.340	1.343	1.342	1.338	1.344
N^3-C^4	1.393	1.381	1.376	1.376	1.384	1.386	1.387	1.383	1.384
C^4-C^5	1.345	1.346	1.346	1.376	1.365	1.361	1.367	1.367	1.364
C^5-N^1	1.369	1.379	1.373	1.378	1.386	1.388	1.384	1.384	1.383
N^3-C^6	1.470	1.467	1.471	1.469	1.740	1.464	1.462	1.477	1.463
N^1-C^7	1.485	1.473	1.477	1.476	1.481	1.472	1.487	1.473	1.472

[a] Ortho stands for orthorhombic form, and mono for monoclinic form. All calculations carried out with a 6-31++G(d,p) basis set.

rotation within the butyl chain. The conformation changes with respect to these torsion angles are complicated, and will be discussed in detail shortly. In all of the conformers obtained, the torsion angle $\tau_3 = C^7-C^8-C^9-C^{10} \approx 180°$.

Nine stable [C_4C_1im]Cl ion pair structures were located and are depicted in Figure 3: these are front (1a, 1b, and 1c), top (2), butside (3a and 3b), methside (4a and 4b), and back (5a). Coordinates of the B3LYP optimized structures are available in the Supporting Information (Table S1). Bond distances around the imidazolium ring for the crystal structure and a selection of the computed conformers are reported in Table 1. The relative stability of each conformer is given in Table 2.

Directly relevant to this study is the work of Turner et al.,[58] who used a stepping stone approach to determine stable structures. Starting with a grid-based search, structures were initially optimized at the HF/STO-3G level, and calculations of an increasing level of sophistication were then initiated (each starting from the lower-level optimized structure); this process culminated with calculations carried out at the MP2/6-31+G(d) level. Turner et al. examined (among other IL pairings) the [C_4C_1im]Cl ion pairs and located three stable structures. As they did not report geometric parameters, it is difficult to make a comparison; however, the most stable at the MP2/6-31+G(d) level appears to be linked to our front-1b structure (0.00 kJ mol^{-1}), their second structure (+1.71 kJ mol^{-1}) appears to be linked to our front-1c, and their third structure (+35.7 kJ mol^{-1}) appears to be linked to our methside-4b structure. The energies of these conformers coincide well with our B3LYP 6-31++G(d,p) results. Turner et al. also noted that their search methodology had some shortcomings,[58] and indeed, it is very difficult to know if we have obtained all the important minima for this ion pair.

TABLE 2: Relative Stability of [C_4C_1im]Cl Conformers Relative to Front-1b Conformer (in kJ mol^{-1})[a]

	B3LYP[b]	HF[c]	MP2[c]
front-1a	0.47	−3.46	9.18
front-1b	0.00	0.00	0.00
front-1c	1.23	−1.12	3.18
top-2	5.60	6.70	3.63
butside-3a	31.15	32.31	32.66
butside-3b	33.74	39.06	31.57
methside-4a	34.24	37.00	42.94
methside-4b	36.29	42.27	39.65
back-5a	60.86	52.68	67.77

[a] All calculations carried out with a 6-31++G(d,p) basis set. [b] B3LYP optimized geometry. [c] MP2 optimized geometry.

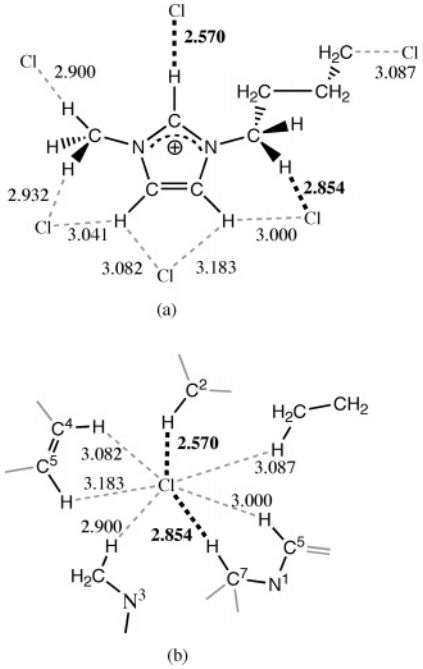

Figure 4. Key cation−anion distances from the orthorhombic polymorph of $[C_4C_1im]Cl$: (a) centered on the cation, (b) centered on the anion. Thick dashed lines indicate possible H-bonds. Structural parameters obtained from Gausview using the CCDC CIF file.[31]

Discussion

The local structure around a single anion or cation has been determined experimentally for the condensed phases. Two crystal structure polymorphs of $[C_4C_1im]Cl$ have been determined and are represented in Figure 4 (orthorhombic) and Figure 5 (monoclinic).[13,31] These structures indicate that in the solid stateanions interact in-plane with the H atoms peripheral to the imidazolium ring, primarily C^2-H and then C^4-H and C^5-H, and show that the anion tends to remain in the ring plane.[13,31] The two monoclinic forms show significant differences in interaction between the cation and the anion.

The liquid-phase structure of $[C_1C_1im]Cl$ has been determined by neutron diffraction. The first maximum in the cation−anion radial distribution function occurs at 4.5 Å (to the center of the imidazolium ring), and each cation is surrounded (on average) by six anions (to within 6.4 Å).[16] The most probable position of the chloride was found to be in a ring around the H bonded to C^2 and above and below the imidazolium ring. Interaction in-plane with the H atoms at C^4 and C^5 ($C^{4/5}-Hs$) was also found. At lower probability levels, the chloride is found in a broad cylinder passing above and below the plane of the imidazolium ring with the methyl groups poking out from the open ends of this cylinder (Figure 4c), and at a much lower probability density broadening of the cylinder toward the methyl groups.[16]

There has been less interest in the existence of weaker cation−anion interactions. Possibilities include interactions between the methylene and the methyl groups of the alkyl chains and the anion ($C^{alkyl}—H\cdots Cl$), interactions between the aromatic imidazolium ring and the anion ($\pi\cdots Cl$), and interactions between the aromatic imidazolium ring and the internal or external alkyl groups ($C^{alkyl}—H\cdots\pi$) or between the aromatic rings of different cations ($\pi\cdots\pi$ stacking effects) or between C^2 on one imidazolium and the ring of a second cation ($C^2—H\cdots\pi$). $C^{alkyl}—H\cdots Cl$ interactions are a possibility in the crystal structures of $[C_4C_1mim]Cl$, the Cl^- anion near $C^5—H$ is shifted toward and possibly interacting with the butyl chain. From neutron diffraction experiments, broadening of the spatial density function from near the alkyl groups is also indicative of an interaction.[16] $C^{alkyl}—H\cdots$anion distances in other ILs have been found to be less than the Wan der Waals radii.[20] $\pi-\pi$ stacking has been observed between the imidazolium rings of some ILs (but not $[C_4C_1im]Cl$), for example, in $[C_4C_1mim]Cl$.[11] A possible $C^{alkyl}—H\cdots\pi$ interaction between the third methylene group of the butyl chain and the imidazolium ring (r = 3.043 Å) has been suggested for $[C_4C_1im]Cl$, which may be blocking possible $\pi-\pi$ stacking.[12] A staggered ion pair ($C^2—H\cdots\pi$) interaction has been proposed for $[C_2C_1im]Cl$ on the basis on NMR experiments.[73] The ability of the Cl^- anion

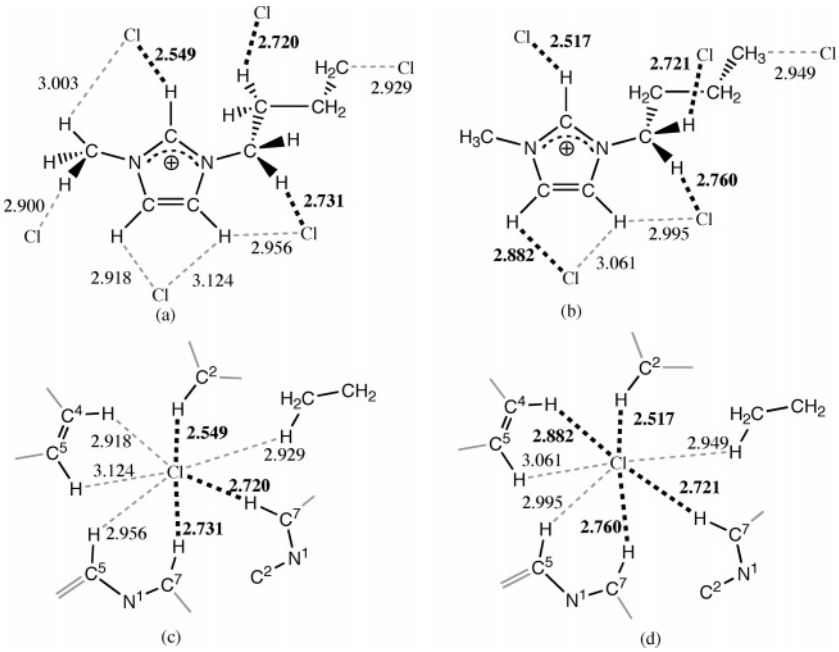

Figure 5. Key cation−anion distances from the monoclinic polymorph of $[C_4C_1im]Cl$. Thick dashed lines indicate stronger H-bonds. Structural parameters obtained from Gausview using the CCDC CIF files. Structure from Holbrey et al. (a) centered on the cation, (c) centered on the anion.[31] Structure from Saha et al. (b) centered on the cation, (d) centered on the anion.[13]

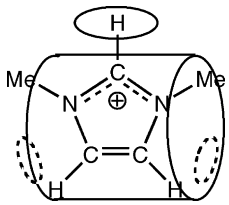

Figure 6. Cartoon of the spatial density map for Cl anion around $[C_1C_1im]^+$ cation from neutron diffraction studies.[16] Dashed lines indicate an area of lesser probability to the side of the "barrel" around the plane of the anion.

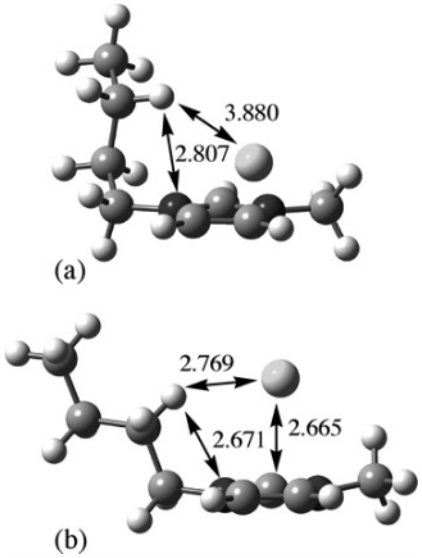

Figure 7. (a) Front-1b and (b) top conformers of $[C_4C_1im]Cl$ showing the position of the Cl anion and distances to C^8-H and C^9-H, respectively.

to participate in or disrupt these secondary interactions will be investigated shortly.

1. Structural Details and the Cl^- Anion Position of B3LYP Optimized Structures. The most stable $[C_4C_1im]Cl$ ion pairs have the Cl^- anion positioned in front of the C^2-H; however, the Cl^- anion is shifted slightly toward the methyl group and lies slightly above (~30°) the plane of the imidazolium ring. This is consistent with the equivalent conformer in the monoclinic crystal structures where the Cl^- anion lies above the plain of the ring. These conformers all form a strong H-bond ($r \approx 2.0$ Å), to the most acidic H (C^2-H) of the imidazolium ring, and a weaker interaction with a hydrogen atom on the methyl group C^6-H ($r = 2.63-2.71$ Å). A similar structure with the Cl^- anion located in front, but positioned on the butyl (rather than methyl) side, was identified at low levels of theory, e.g., HF/3-21G; however, the stability of this structure was eroded at higher levels of theory, indicating that calculations at lower levels of theory may not be predictive for this system. Similar concerns have been raised elsewhere.[58]

Lying approximately 5 kJ mol^{-1} above the front conformers is the top-2 conformer. Here, the Cl^- anion lies above the C^2-H bond, sitting closer to the hydrogen (2.648 Å) than C^2 (2.665 Å) and with a $H-C^2-Cl$ angle of 90.96°. This isomer differs significantly from all the other conformers (except back-5a) in that no strong H-bonding interactions are present. The butyl chain is also significantly distorted, twisting up toward the Cl^- anion, and C^8-H (rather than C^9-H as in the front conformers) is rotated toward the Cl^- anion (Figure 7). Examination of the structure shows that the C^8-H is positioned almost directly above N^1. No Cl^- anion is found lying above the imidazolium ring in the crystal structure; however, this conformer is ~30 kJ/mol lower in energy than the butside conformer, which is observed in the crystal structure.

There is the possibility of a $Cl^-\cdots\pi$ (imidazolium ring) interaction for the top conformer. The imidazolium cation is known to be capable of forming $\pi\cdots\pi$ interactions, as these have been observed in the crystal structures of other ionic liquids.[11] No evidence for a $Cl\cdots\pi$ interaction was found in total electron density plots; however, a small interaction of this type can be identified in the HOMO (Cl interaction with the $C^4=C^5$ bond) and HOMO − 3 (Cl interaction with the delocalized 3c-4e $N^1-C^2-N^3$ bond). The ring Cl^- anion position inferred from the neutron diffraction studies of $[C_1C_1im]Cl$ indicates that the top conformer is viable in the liquid phase.[16]

The butside conformers are ~30 kJ mol^{-1} higher in energy than the front conformers. At the B3LYP level, the butside-3a is more stable than the butside-3b conformer, but this is reversed at the MP2 level; however, the energy differences are only on the order of a few kilojoules per mole (Table 2). Both conformers form a weak H-bond with C^5-H of the imidazolium ring ($r \approx 2.18$ Å). The Cl^- anion remains essentially in-plane with the imidazolium ring, as the out-of-plane torsion angle is less than 10°. In comparison to front-1a ($\tau_1 = -58°$), the butyl chain in butside-3a has rotated slightly to accommodate a weak and long-range interaction between the Cl^- anion and the second methylene unit (C^7-H; $\tau_1 = -94°$). The position of the butyl chain in butside-3b also differs significantly from that in front-1b. In the "b" conformers, the methylene units reorientate to tilt toward the Cl^- anion; in front-1b, this means tilting toward the front of the molecule ($\tau_1 \approx -36°$), and in butside-3b, this means tilting toward the back of the molecule ($\tau_1 \approx -74°$); moreover, in each case, the H atoms are oriented on different sides of the carbon backbone.

The methside conformers are ~3 kJ mol^{-1} less stable than the butside conformers. At the B3LYP level, the methside-4a is more stable than the methside-4b conformer, but this ordering is reversed at the MP2 level. However, the energy differences are only on the order of a few kilojoules per mole; Table 2. The primary H-bond interaction of the Cl^- anion is with C^4-H, and a secondary longer-range interaction occurs with C^6-H, which has rotated relative to its position in the front conformers to enable the H-bond to form. A calculation was set up with the methyl group rotated such that there were two potential $C^6-H\cdots Cl$ interactions; however, this structure reoriented immediately, indicating a preference for the single, stronger H-bond. The Cl^- anion remains essentially in-plane with the imidazolium ring, and as there is no potential for interaction with the butyl chain, the torsion angles τ_1 and τ_2 remain very similar to those of the front conformers.

The back conformer is ~60 kJ mol^{-1} higher in energy than the front conformers. The Cl^- anion remains essentially in-plane with the imidazolium ring; $Cl-H-C^4-C^5 = -1.2°$. Two H-bonding interactions occur, and in contrast to the crystal structures, the Cl anion lies slightly closer to the butyl C^5-H than the C^4-H; $C-H\cdots Cl$ distances are 2.526 and 2.578 Å, respectively. In the crystal structure, the Cl^- anion is also H-bonding to other cations. It appears that this site offers a modicum of additional stabilization after the formation of a primary H-bond. Car−Parrinello MD calculations show no presence of the Cl^- anion in this region.[32] Moreover, Hardacre et al. using neutron diffraction do not find the Cl^- anion in this region either (Figure 4c).[16,17] However, classical studies find a significant probability for this site to be occupied; Liu et al. obtained a slightly smaller probability than Hanke et al.[18,33] This

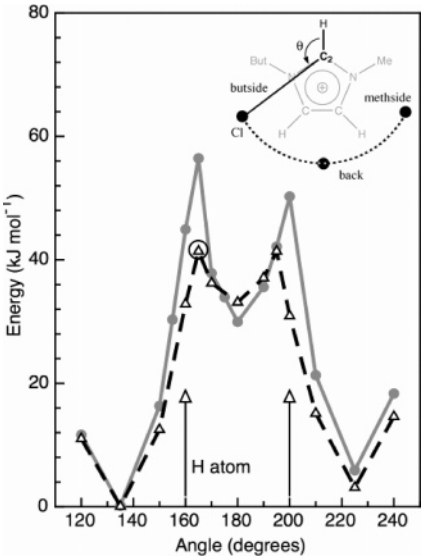

Figure 8. Scan of the potential energy surface moving the Cl^- anion in an arc "behind" the imidazolium ring. C^2-Cl distance is kept fixed, and the angle θ varied in 15° intervals from 120° to 240°. Closed circles with a solid line are HF/3-21+G(d), and open triangles with dashed line are B3LYP/6-31++G(d,p) level results. The circled point could not be optimized and has been estimated.

is all the more surprising, because the same charges were used in fitting the neutron diffraction data as in the simulation of Hanke et al.[16,18] The difference in probability between the front and the butside (and methside) sites, which is linked to a 30 kJ mol^{-1} difference in energy, could be expected to generate a similar level of loss in probability at the back site which is another 30 kJ mol^{-1} higher in energy, and this is not evident in the classical simulations.

Converging the back conformer was very difficult and was only established after scanning the potential energy surface "behind" the imidazolium ring, Figure 8. The scan was initially performed at the HF/3-21+G(d) level with the C^2-Cl distance fixed at 5.048 Å (that for the optimized butside structure at HF/3-21+G(d) level); the Cl^- anion was forced to remain coplanar with the imidazolium ring, the $H-C^2-Cl$ angle θ was fixed at 15° intervals between 120° and 240°, and all other geometric parameters were optimized. The optimized structures were used to initiate optimizations at the B3LYP/6-31++G(d,p) level with C^2-Cl fixed at 5.0 Å (that of the optimized butside structure); all other geometric parameters were optimized. Interestingly, the HF/3-21+G(d) calculations performed nearly as well as B3LYP/6-31++G(d,p) level calculations. Minima are clearly identified for the butside, back, and methside conformers; however, the back conformer is only stabilized by ~10 kJ mol^{-1} at the B3LYP level. Barriers (~40 kJ mol^{-1} at B3LYP level relative to the butside conformer) occur when the Cl^- anion is roughly in line with the $C^{4/5}$ hydrogen atoms.

2. Hydrogen Bonding. It is now well-established that cation−anion H-bonding occurs in some imidazolium-based ionic liquids (however, the results for anions such as $[PF_6]^-$ are still inconclusive).[3,9,10,15,74] Characterizing these interactions is problematic, because hydrogen bonding can span a wide range of energies and distances. Jeffrey, for example, has used as criteria for a "normal" O···H H-bond: H···O < 2.7 Å and C−H···O > 90°.[75] Alternatively, a criterion that the interaction distance be less than the sum of the respective van der Waals radii has also been used.[76] Using van der Waals radii of H = 1.20 Å and Cl = 1.75 Å[77] gives a H-bond maximum distance of 2.95 Å (Cl). This is significantly longer than the standard cutoff for

TABLE 3: Cation−Anion H-Based Interactions for the $[C_4C_1im]Cl$ Ion Pair[a]

	strong		weak		ring
	H	r	H	r	r
front-1a	$C^2-H\cdots Cl$	1.995	$C^6-H\cdots Cl$	2.704	
front-1b	$C^2-H\cdots Cl$	2.004	$C^6-H\cdots Cl$	2.717	2.808
front-1c	$C^2-H\cdots Cl$	2.002	$C^6-H\cdots Cl$	2.635	2.806
top-2			$C^2-H\cdots Cl$	2.564	
			$C^6-H\cdots Cl$	2.721	
butside-3a	$C^5-H\cdots Cl$	2.176	$C^7-H\cdots Cl$	2.497	
butside-3b	$C^5-H\cdots Cl$	2.175	$C^7-H\cdots Cl$	2.406	2.804
methside-4a	$C^4-H\cdots Cl$	2.161	$C^6-H\cdots Cl$	2.348	
methside-4b	$C^4-H\cdots Cl$	2.164	$C^6-H\cdots Cl$	2.354	2.823
back-5a			$C^5-H\cdots Cl$	2.526	
			$C^4-H\cdots Cl$	2.578	

[a] Strong (r < 2.3); weak (2.3 < r < 2.75); ring is the distance between the closest H at C^9 of the butyl chain and N^1 of imidazolium ring. r is given in angstroms.

biological H-bonds of r < 2.0 Å; however, there is ample evidence for weaker (and longer) H-bonds based around a C−H···A interaction, where A = O, N, S, a halide, or the π-electrons of olefins or aromatics, particularly if the carbon is activated by an electronegative substituent.[78] Defining a H-bond is difficult. In the following, we have used purely geometric criteria and assigned an interaction as a strong H-bond if the C−H···Cl distance r < 2.3 Å, and a weak H-bond if 2.3 < r < 2.75 Å. The maximum distance is thus shorter than the van der Waals radii limit for a H-bond. The existence and type of H-bonds that exist for the various ion pair configurations is examined and related to the computed vibrational spectrum. IR and Raman spectroscopy have been used in the past to verify the existence of H-bonds in ionic liquids.[9,15,79,80]

Key H-bonding anion−cation distances are summarized in Table 3. H-bonding distances obtained from the crystal structure of $[C_4C_1im]Cl$ are shown in Figure 4. In addition, there is the possibility of an interaction between a butyl chain methylene H and the imidazolium ring, and where relevant, the appropriate $C^{butyl}-H\cdots N^1$ distances have also been reported in Table 3. The existence, or not, of an intramolecular $C^{butyl}-H\cdots\pi$ interaction will be discussed in more detail shortly.

For each of the front, butside, and methside conformers, the Cl^- anion prefers to form two basic types of interaction: a shorter-range hydrogen bond to an imidazolium ring H atom (Cl···H distances range from 2.00 to 2.18 Å) and a weaker interaction with a H atom from one of the alkyl groups. Both interactions are important, as no stable conformer with only one H-bonding interaction was found. The back and top conformers form a different kind of arrangement; there is no short H-bond, but two weaker H-interactions form. In the top conformer, an additional more diffuse interaction may also occur, as $r(C^8-H\cdots Cl)$ = 2.77 Å.

In the gas phase, each ion interacts only with one anion, while in the liquid and solid phases, each ion interacts with multiple ions of opposite charge, and hence, the tightest H-bonds in the crystalline (2.52 Å) and liquid phases (2.78 Å) are generally longer than those found for the gas-phase ion pairs (2.10 Å). However, it appears that the longer-range H-bond interactions are less influenced by the phase change. For example, in the crystal structure of $[C_1C_1im]Cl$, H···Cl distances lie between 2.62 and 2.73 Å,[81] and in the crystal structure of $[C_4C_1im]Cl$, H···Cl distances lie between 2.52 and 2.88 Å,[13] while in the gas-phase structures, these weaker H-bonds lie between 2.5 and 2.75 Å. Classical calculations on liquid $[C_2C_1im][AlCl_4]$ at 298 K indicate that slightly longer H-bonds are formed; H···Cl distances lie between 2.83 Å and 2.98 Å.[36]

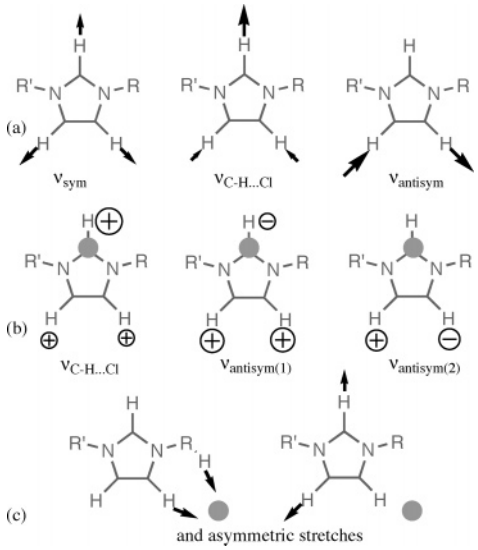

Figure 9. Key C^{ring}−H vibrations for the (a) $[C_4C_1im]^+$ cation, (b) top $[C_4C_1im]Cl$ ion pair, and (c) butside and methside ion pairs.

TABLE 4: Key in-Plane C−H Vibrational Frequencies (cm^{-1}) at the B3LYP/6-31++G(d,p) Level of Theory[a]

	$\nu_{(C-H\cdots Cl)}$	$\Delta\nu$	ν_{sym}	ν_{asym}
cation	3298		3312	3295
cation[b]	3176		3189	3173
front	2655	−643	3308	3290
top	3336	+38	3314	3296
butsid	2918(a)	−380	3302	3299
	3011(s)	−287		
methside	2902(a)	−338	3304	3297
	2960(s)	−396		
back	3295	−55	3257	3230
		−63		

[a] $\Delta\nu = \nu_{ion\ pair} - \nu_{cation}$ for the relevant mode. [b] Scaled by 0.963.

3. IR Vibrations. Frequency analysis within the harmonic approximation has been performed for all the optimized B3LYP structures (Supporting Information Tables S2 (cations) and S3 (ion pairs)). The computed C−H stretching modes for the isolated $[C_4C_1im]^+$ cation lie in the region of 3019−3313 cm^{-1}. Vibrations in conformers with different butyl chain orientations differ by less than 3 cm^{-1}, and thus, averaged values have been reported. The three highest-energy C−H stretching vibrational modes associated with the C^{ring}−H bonds are shown in Figure 9a; they include the symmetric stretch (3312 cm^{-1}), a mode that is primarily a C^2−H stretch (3298 cm^{-1}), and the $C^{4/5}$−H antisymmetric stretch (3295 cm^{-1}). The computed vibrational frequencies related to H-bonding for the cation and ion pair conformers are presented in Table 4. It is typical for calculations of this type to overestimate vibrational modes; however, scaling factors are basis set dependent, and to the best of our knowledge, no scaling factor has been published for the 6-31++G(d,p) basis set, and thus, these results are reported without correction.[82] A scaling factor of 0.963 has been proposed for the B3LYP/6-31G(d) method; applying this scaling factor to the cation vibration leads to a correction of ∼150 cm^{-1} (Table 4).[83]

In comparison to the monomer, the $[C_4C_1im]Cl$ ion pair has three additional vibrations; these are associated with the primary C−H···Cl interaction. However, the fundamentals are not isolated, but appear in combination modes. Formation of the H···Cl bond is expected to weaken the C−H bond and produce a shift to lower frequency, or red shift, in the associated C−H stretching modes. The C−H bond affected will depend on the position of the chloride anion. For each of the ion pair conformers, the C^{ring}−H modes not involved in H-bonding should remain similar to those of the cation.

TABLE 5: Key Out-of-Plane C−H Vibrational Frequencies (cm^{-1}) at the B3LYP/6-31++G(d,p) Level[a]

	$\nu_{(C-H\cdots Cl)}$	$\Delta\nu$	$\nu_{asym(1)}$	$\nu_{asym(2)}$
cation	829		751	830
top	727	−102	645	830

[a] $\Delta\nu = \nu_{ion\ pair} - \nu_{cation}$ for the relevant mode.

There is a large red shift (643 cm^{-1}) in the C^2−H stretch frequency for the front conformers to ∼2655 cm^{-1} (averaged over the 1a, 1b, and 1c conformers) and an associated large increase in intensity. As anticipated, the $C^{4/5}$−H stretching modes of the front and top conformers remain similar to those of the cation; the $C^{4/5}$−H modes of the back-5 conformer are however only lightly affected by the presence of the chloride anion. The top-2 conformer has similar in-plane modes to the cation; however, the C^2−H stretch frequency is blue-shifted by 38 cm^{-1}; Table 4. The Cl^- anion also affects out-of-plane motions in this conformer (Figure 9b, Table 5) where the expected red shift is actually observed for the C^2−H out-of-plane mode, and one even larger (−106 cm^{-1}) is determined for the antisymmetric mode (asymm(2) in Figure 9b). However, the extremely large intensity enhancement observed for the front conformers is not found.

Talaty et al. have examined the IR and Raman spectra of the ionic liquid and computed (at the B3LYP/6-311+G(2d,p) level) the vibrational spectrum of $[C_nC_1im]PF_6$ ($n = 2, 3, 4$).[52] A single $[C_4C_1im]PF_6$ structure was examined where the PF_6^- anion was located to the front and above the imidazolium ring. The computed $\nu(C^{4/5}$−H) stretches were located at 3277 and 3294 cm^{-1}, and are ∼20 cm^{-1} less than those obtained by us for the isolated cation. The computed $\nu(C^2$−H) stretch was found at 3270 cm^{-1} and exhibits a minor red shift in comparison to the cation. This is in contrast to the $[C_4C_1im]Cl$ front conformers, which exhibit a large red shift, and the top conformers, which exhibit a small blue shift, indicating that H-bonding is significantly weaker in the $[C_4C_1im]PF_6$ ion pair.

The butside-3 and methside-4 conformers have four important modes due to participation from the adjacent alkyl group; the relevant symmetric modes are represented in Figure 9c; there will also be the associated asymmetric modes. The C^5−H stretch dominates the antisymmetric mode for the butside ion pairs; however, both C^4−H and C^6−H contribute equally for the methside ion pairs. The difference in contribution is reflected in the (average) intensity enhancement of these modes: butside, 691(a) and 230(s); and methside, 649(a) and 605(s). Both the symmetric and antisymmetric modes exhibit a significant red shift. The nearly equal participation in the methside ion pair of C^4−H and C^6−H in the stretch indicates that two roughly equivalent H-bonds are formed. A similar situation is found for the butside-3b ion pair. However, participation of C^7−H is significantly less than that of C^5−H for the butside-3a ion pair, indicating that no strong H-bond is forming, and thus implies a bond distance cutoff for the formation of a viable secondary H-bond; $r(C^7$−H···Cl) = 2.50 Å is too long in butside-3a, while in butside-3b, $r(C^7$−H···Cl) = 2.41 Å, a weak H-bond forms.

These computational results are qualitatively consistent with previously reported IR spectra of similar ILs; however, as our results have not been scaled, they are high. For example, the $[C_2C_1im]$halide ILs have a ν(C−H) stretch at 3200−3000 cm^{-1}, slightly lower but in line with the unaffected C^{ring}−H modes at 3290−3310 cm^{-1} computed here.[9] A new peak observed between 3050 and 3080 cm^{-1} is consistent with computed

TABLE 6: Butyl Chain Torsion Angles $\tau_1 = C^2-N^1-C^7-C^8$ and $\tau_2 = N^1-C^7-C^8-C^9$ (in degrees) and Relative Stability (in kJ mol^{-1}) for the Front Conformers of the $[C_4C_1im]^+$ Cation[a]

	B3LYP			MP2			HF
	τ_1	τ_2	E^b	τ_1	τ_2	E^c	E^c
cation-a	−102	180	0.0	−103	179	3.71	0.00
cation-b	−83	−65	2.69	−73	−58	1.92	5.30
cation-c	−108	+64	1.01	−108	+59	0.00	2.54

[a] All calculations carried out with a 6-31++G(d,p) basis set. [b] B3LYP optimized geometry. [c] MP2 optimized geometry.

H-bonding modes for the $[C_4C_1im]Cl$ methside ion pair at 2902 and 2960 cm^{-1}. An observed reduction in the peak intensity at 3130 cm^{-1} is consistent with the formation of front and methside conformers (which no longer have a mode at this wavenumber) and the continuing presence of top and back conformers (which show little variation in the C^2-H mode). A series of weak absorptions have between observed in the experimental spectra between 2500 and 2850 cm^{-1} and assumed to arise from anharmonic effects.[9] However, as the present analysis was carried out within the harmonic approximation, it is possible that these bands are evidence of the formation of a small amount of the front conformer, small because the front ion pair is computed to have a very intense mode at ∼2655 cm^{-1}. Spectra of $[C_2C_1im]Cl-AlCl_3$ ILs exhibit imidazolium-based bands between 3150 and 3200 cm^{-1} and a broad red-shifted peak at 3118 cm^{-1} due to C^2-H, again consistent with the results reported here. Moreover, deuteration experiments indicated that the Cl^- anion interacts with all three ring hydrogen atoms.[84]

4. Butyl Chain Rotation. It is clear from the existence of multiple stable structures that rotation of the alkyl chain is important. Several questions arise: How free is the rotation of the butyl chain in the cation? What effect does the presence of a Cl^- anion have on this rotation? Turner et al. found the potential energy surface extremely flat for rotation of the ethyl chain in the $[C_2C_1im]Cl$ cation.[58] Urahata and Ribeiro (Figure 7 of their paper) have shown that there is significant movement of the alkyl chains in the liquid phase.[19] Recently, there has been crystallographic evidence for disorder associated with multiple orientations of the butyl chain, which remains roughly in-plane, or bends up or down beyond the first CH_2 unit.[11] In addition, two polymorphs which have different butyl chain orientations have been found for $[C_4C_1im]Cl$.[31] Most classical force fields have been based on a single conformer of the imidazolium cation. However, an average of partial charges over several minimum-energy structures may be more suitable than those obtained for a single configuration. One force field has already been developed along these lines, taking an average from two geometries.[41] How many low-lying structures of importance are there? Identifying the principle low-lying structures and the effects of correlation on the relative energy ordering of these will allow for informed decisions to be made with respect to force field parametrization of the imidazolium cation.

The orientation of the butyl chain has been examined in detail for the isolated cation and for the front ion pair conformers. Structures with similar orientations have been obtained for the methside and butside conformers, and hence will not be discussed in detail. Three local minima are found for the isolated cation; Table 6. Cation-a resembles the imidazolium cation found in the monoclinic crystal structure of $[C_4C_1im]Cl$ where there are four symmetry-related ion pairs with $\tau_1 = \pm 83°$ and $\tau_2 = \pm 174°$. Cation-b and cation-c resemble the imidazolium cations found in the orthorhombic crystal structure of $[C_4C_1im]Cl$ where there are four symmetry-related ion pairs with $\tau_1 = \pm 79°$ and $\tau_2 = \pm 68°$.[13,31] The butyl chains of cation-b and cation-c fold above the imidazolium ring, allowing C^9-H to lie above N^1; the $H\cdots N$ distance is ∼2.81 Å in both cases. Dupont et al. have observed a similar interaction in the crystal structure of $[C_4C_1im][B(Ph)_4]$, which they attributed to a $C-H\cdots\pi$ (aromatic ring) interaction, and noted a $C^9-H\cdots\pi$ distance of 3.043 Å (to the center of the ring).[12] If such an interaction does occur (see below for reasons why it may not), it may be why no $\pi\cdots\pi$ stacking is observed in the crystal structure of $[C_4C_1im]Cl$. $\pi\cdots\pi$ stacking has been observed in other related ionic liquids, for example, $[C_2C_1im]Cl\cdot H_2O$ and $[C_4C_1mim]Cl$.[11]

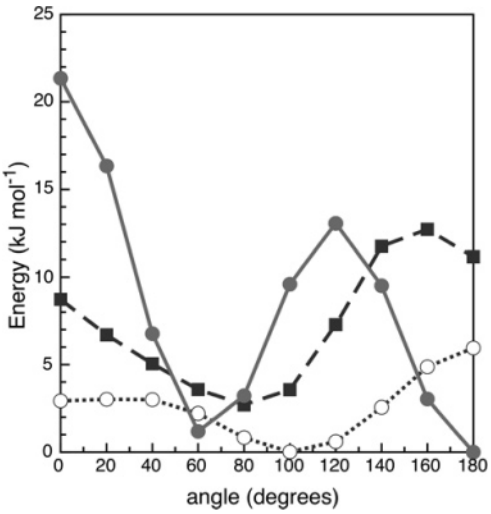

Figure 10. Energy profile for rotation about the (absolute) torsion angles τ_1 and τ_2, calculated at the B3LYP/6-31++g(d,p) level for the isolated $[C_4C_1im]^+$ cation. Rotation about τ_2 = solid line with closed circles. Rotation about τ_1 (τ_2 initially ≈ 180°) = dotted line with open circles. Rotation about τ_1 (τ_2 initially ≈ −60°) = dashed line with closed squares.

Rotation about the two torsion angles, $\tau_1 = C^2-N^1-C^7-C^8$ and $\tau_2 = N^1-C^7-C^8-C^9$, has been examined for both the isolated $[C_4C_1im]^+$ cation and the ion pair front ion pair. In the case of the isolated cation, there is a single minima for rotation about τ_1 and double minima for rotation about τ_2; Figure 10. The angles were scanned at 20° intervals between 0° and 180° at the B3LYP/6-31++G(d,p) level. To ensure that the enforced rotation occurred only in the butyl chain and did not deform the ring C^2-H, two torsion angles, $H-C^2-N^1-C^7$ and $C^6-N^3-C^2-H$, were initially frozen (at their optimized values), and all other geometric parameters were optimized. Then, in a second set of calculations, the torsion angles, $H-C^2-N^1-C^7$ and $C^6-N^3-C^2-H$, were released and all the geometric parameters allowed to optimize.

Rotation about τ_2. Rotation through τ_2 generates a barrier at 0° and another at 120°; these barriers are due to eclipse of the significant substituents at C^7 and C^8 (Figure 11a), and hence, when these substituents are staggered, there are minima (see Figure 11), for example, at $\tau_2 \approx 180°$ (cation-a), −60° (cation-b), and +60° (cation-c). The computed barriers to rotation are not high (<20 kJ mol^{-1}); the relative stability of these $[C_4C_1im]^+$ cation conformers are presented in Table 6. An anti-periplanar conformation is found for the C^8-C^9 bond; in two structures, this arrangement requires one of the C^9-H to align above N^1 closer to C^2 (cation-b) or C^5 (cation-c), (Figure 11b). Hence, there are better reasons than the presence of a $C-H\cdots N$ or $C-H\cdots\pi$ interaction to explain the position of hydrogen atoms directly above N^1. Interactions of this type ($X\cdots\pi$) are generally only well-reproduced by calculations that include significant correlation (i.e., MP2); the reversal in the stability

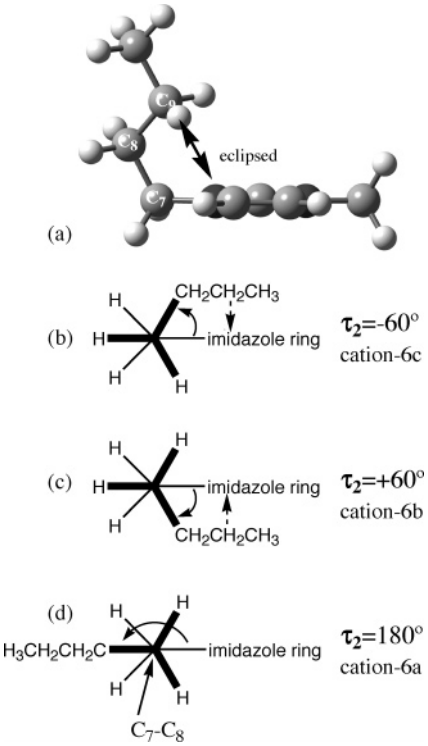

Figure 11. $[C_4C_1im]^+$ cation. (a) gives the structure with $\tau_2 = 0°$ (unstable) showing steric effects, and (b)−(d) show the staggered conformers.

of these conformers on the inclusion of more correlation indicates that the C−H···π interaction may be making a small contribution to conformer stability. In summary, rotation about τ_2 is primarily governed by steric effects, with the possibility of a modicum of stabilization (<2 kJ mol^{-1}) obtained through very weak C−H···π type interactions.

Lopes et al. have used HF/6-31G(d) geometries and single-point energy computations at the frozen core MP2 level using a cc-pVTZ basis set with all f functions removed to scan the potential energy surface for rotation about τ_2; they obtained a conformer ordering similar to our fully optimized MP2 (frozen core) level calculations (global minimum at $\tau_2 \approx 60°$ and $E(\tau_2 \approx 180°) = +2.00$ kJ/mol).[41]

Rotation about τ_1. Rotation about τ_1 must be considered for each of the τ_2 local minima (Figure 10). Rotation in the $\tau_2 \approx 180°$ well is essentially free, and barriers are only slightly higher for the $\tau_2 \approx -60°$ well. These barriers are steric in origin and arise from repulsion between $C^{2/5}$−H of the ring and C^8−H of the butyl chain (Figure 12). The accuracy of two lower-level methods (B3LYP/3-21+G(d) and HF/6-31G(d)) has been tested by performing scans over τ_1 (Supporting Information Figure S1). The B3LYP/3-21+G(d) method cannot accurately represent the local potential energy surface; barrier heights were underestimated, and a nonexistent local minimum was predicted for $\tau_1 = 0.0°$. The HF/6-31G(d) method performed better, reproducing the local shape of the potential energy surface well but overestimating barrier heights. Performing single-point calculations at a higher level, however, can rectify this deficiency.

Presence of Cl$^-$ Anion. We are not only interested in rotation of the butyl chain in the isolated imidazolium cation, but also in the ion pair complex; the effect of the Cl$^-$ anion on the torsion around τ_1 is shown in Figure 13. The barrier to rotation is reduced at angles less than 80° and even deepened for the $\tau_2 = 60°$ well, but increased at larger angles. The presence of the Cl$^-$ anion has also flattened the bottom of the $\tau_2 \approx 180°$

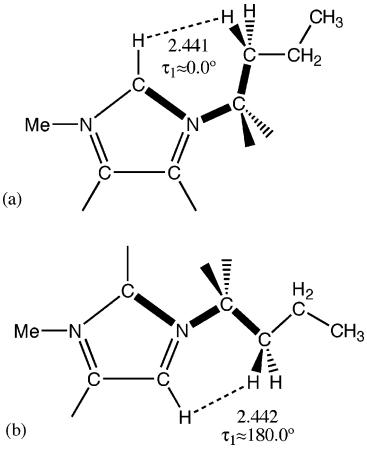

Figure 12. $[C_4C_1im]^+$ cation: structure with (a) $\tau_1 = 0°$ and (b) $\tau_1 = 180°$, showing steric effects.

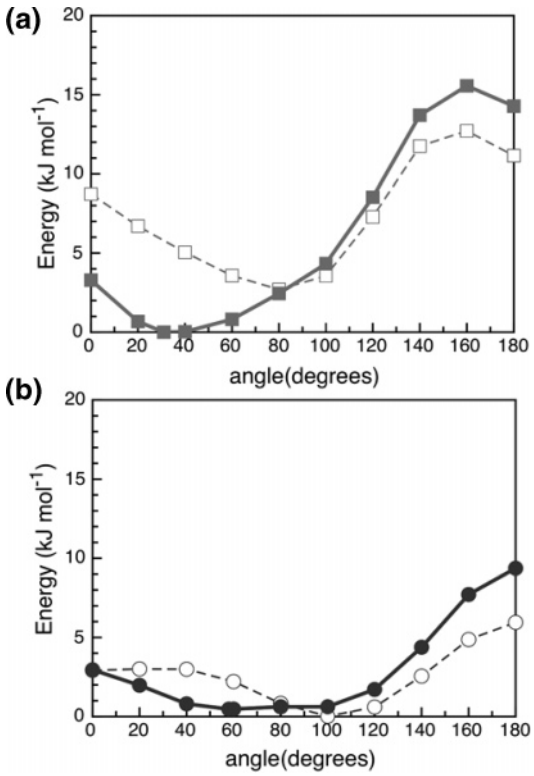

Figure 13. Effect of the Cl anion on the energy barriers to torsional rotation (absolute angles reported) about τ_1 for both (a) $\tau_2 \approx -60°$ cation = open squares with dashed line, and $[C_4C_1im]Cl$ = closed squares with solid line (the minimum structure is front-1b (and related to front-1c)) and (b) $\tau_2 \approx 180°$ cation = open circles with dashed line, and $[C_4C_1im]Cl$ = closed circles with solid line (the minimum structure is front-1a).

potential energy well, allowing the butyl chain to rotate more freely over an extended region from $\tau_1 \approx -100°$ to $+100.0°$. Thus, to obtain a bona fide global minimum, optimization must be carried out under very tight convergence criteria. At the MP2 level, the isolated cation is stable at $(\tau_1, \tau_2) = (-73°, -58°)$ but is significantly less twisted in the ion pair $(\tau_1, \tau_2) = (-38°, -60°)$ because of the presence of the Cl$^-$ anion (in the front position). In summary, rotation is enhanced, potential wells become flatter, and low angle barriers are reduced; however, full rotation is inhibited slightly by the presence of the Cl$^-$ anion.

5. Energy Ordering of the Conformers. *ZPE and BSSE Corrections*. Small energy differences were obtained between the front and top conformers, indicating that zero point energies

TABLE 7: Relative Stability of [C_4C_1im]Cl Conformers Relative to Front-1a (in kJ mol^{-1})[a]

	ΔE	ΔE_{ZPE}	ΔE_{BSSE}	ΔE_c
front-1a	0.00	0.00	0.00	0.00
front-1b	−0.48	0.78	0.13	0.43
front-1c	0.76	0.19	0.05	1.00
top-2	5.13	1.52	0.24	6.89
butside-3a	30.69	0.38	0.01	31.07
butside-3b	33.27	0.75	0.07	34.08
methside-4a	33.78	0.25	−0.16	33.87
methside-4b	35.82	0.61	−0.14	36.29
back-5a	60.39	0.05	−0.13	60.31

[a] ΔE is the energy difference; ΔE_{ZPE} is the energy difference in the zero-point energy correction; ΔE_{BSSE} is the energy difference in the basis set superposition error. $\Delta E_c = \Delta E + \Delta E_{ZPE} + \Delta E_{BSSE}$ at the B3LYP/6-31++G(d,p) level.

TABLE 8: Relative Stability of [C_1C_1im]Cl Isomers (in kJ mol^{-1})[a]

	B3LYP	BPE	MP2	DP
front-6	0.00	0.00	1.79	13.51
top-7	4.52	3.59	0.00	0.00
methside-8	33.78			
back-9	61.60			

[a] Structures are identified by the position of the anion. All our calculations use a 6-31++G(d,p) basis set. DP = calculations by Del Pópolo et al.

(ZPE) and basis set superposition errors (BSSE) may alter which is the most stable conformer. ZPE for the ion pairs is substantial, ~592 kJ mol^{-1} (Supporting Information Table S4), but varies only slightly between conformers. The BSSE is only on the order of 1 kJ mol^{-1} (Table S4), and also varies only slightly between conformers. These corrections and the final energy differences are documented in Table 7. ZPE and BSSE corrections change the most stable conformer at the B3LYP/6-31G++(d,p) level from the front-1b to the front-1a conformer; the top-2 conformer still lies more than 5 kJ mol^{-1} above the lowest-energy front conformer. The combined effect of ZPE and BSSE corrections is less than 2 kJ mol^{-1} (at the B3LYP/6-31G++(d,p) level). The energy of formation for the ion pair pairs ranges from −314.69 kJ mol^{-1} (back-5a) to −375.55 kJ mol^{-1} (front-1b) at the B3LYP/6-31G++(d,p) level (Table S4); this is substantial, but unsurprising given the negligible vapor pressure of the ionic liquid.

Front vs Top Conformers. The top-2 conformer of [C_4C_1im]Cl lies above the front-1 conformer by ~5 kJ mol^{-1} at the B3LYP/6-31G++(d,p) level. However, Del Pópolo et al., using Car−Parrinello MD to study [C_1C_1im]Cl, found that the top conformer lies 13.51 kJ mol^{-1} below the front conformer.[32] To establish if this reversal is due to the longer alkyl group in [C_4C_1im]Cl, several stable conformers of [C_1C_1im]Cl have been calculated at the B3LYP/6-31++G(d,p) level (minima confirmed by frequency analysis); Table 8 and Supporting Information Figure S2. Results consistent with our [C_4C_1im]Cl calculations were obtained: The front-6 conformer of [C_4C_1im]Cl is more stable than the top-7 conformer (by 4.52 kJ mol^{-1}). Several structural features of the top conformer also differ from those obtained by Del Pópolo et al. (see, for example, the entries in Table 9). The calculation was repeated with the PBE functional[68] used by Del Pópolo et al., and again, the front-6 isomer was found to be more stable (by 3.59 kJ mol^{-1}). However, at the MP2 level, the stability is reversed: The top-7 [C_1C_1im]Cl ion pair becomes the most stable, but only by 1.79 kJ mol^{-1}, much less than the 13.7 kJ mol^{-1} predicted by Del Pópolo et al. We note that there are substantial differences between the two sets

TABLE 9: Key Bond Distances (Å) and Angles (deg) of the Top-7 [C_1C_1im]Cl Ion Pair[a]

	B3LYP	MP2	DP
top C···Cl	2.665	2.712	2.20
top Cl−C−H	77.46	86.09	93.2
front H···Cl	1.990	2.008	1.74
front C−H	1.11	1.1114	1.2
front Cl−C−H	159.93	157.78	159.0

[a] All our calculations use a 6-31++G(d,p) basis set. DP = calculations by Del Pópolo et al.

of calculations: gas phase vs periodic boundary conditions, no pseudo-potentials vs the use of pseudo-potentials, Gaussian basis sets vs plane-wave basis sets. Nevertheless, it is disappointing that these two sets of calculations do not converge, and we are currently investigating why this might be so.

The preference of the Cl^- anion for a front vs top conformation is also difficult to elucidate in the condensed phase. For example, Urahata and Ribeiro, using classical methods (liquid phase), have found that the anion prefers to lie above and below the plane of the imidazolium ring; they also found that the F^- anion prefers to lie close to the acidic C^2−H, the Cl^- anion smears out over the C^2−H bond region, and a Br^- anion prefers to be over the ring.[19] However, neutron diffraction data (liquid phase) show that the Cl^- anion in [C_1C_1im]Cl prefers to remain in a ring around the C^2−H, while similar data for [C_4C_1im][PF_6] show the anion preferring a position above and below the center of the imidazolium ring.[16,17] Li et al. using classical simulations found the most probable position of the Cl^- or PF_6^- anions to be above and below C^2.[33] The position of the anion is clearly very sensitive to the charge density of the anion (F^- and Cl^- being relatively more charge dense than Br^-, I^-, and PF_6^-). This indicates that the Lennard-Jones parameters for the anion must be chosen with particular care.

Density functional methods are unable to recover dispersion effects, which may be significant for this ion pair system. Moreover, higher-level calculations are required to establish the most stable conformer and to establish the relative accuracy of B3LYP method. In Table 2, HF and MP2 level energies (calculated using optimized MP2 geometries) were reported alongside the B3LYP results. Including correlation does not change the relative ordering of conformers with respect to the Cl^- anion positions, but it does have an effect on which butyl chain rotomer is the most stable; the B3LYP method overestimates the stability of the front-1a conformer. Moreover, the relative energy of the top conformer decreases significantly when including correlation. More accurate calculations for the lowest-energy (front and top) conformers were carried out and are reported in Table 10.

Changing the basis set has a significant effect on the MP2 level calculations; the relative energy ordering between the conformers is retained, however; the cc-VDZ basis set appears to overestimate the energy of the top-2 conformer by ~15 kJ mol^{-1}. Increasing the amount of correlation recovered at the CCSD and CCSD(T) levels for the cc-pVDZ basis set does not improve the situation. These calculations are very expensive, and insufficient resources were available to test a cc-pVTZ basis set. However, using an aug-cc-pVDZ basis set at the MP2 level significantly stabilizes the top-2 conformer, and recovering further correlation at the CCSD(T) level indicates that the top-2 conformer is slightly (<1 kJ mol^{-1}) more stable than the front-1b conformer. Hence, at the highest level available to us, the top and front conformers are essentially degenerate. These results indicate that correlation and basis set effects are important for the top-2 conformer (where there is the possibility of a Cl···π

TABLE 10: Relative Stability of Key [C_4C_1im]Cl Conformers Relative to Front-1b (in kJ mol^{-1})[a]

	B3LYP 631++G(d,p)	MP2 631++G(d,p)	MP2 cc-pVDZ	CCSD cc-pVDZ	CCSD(T) cc-pVDZ	MP2 aug-cc-pVDZ	CCSD(T) aug-cc-pVDZ
front-1a	0.48	9.18	9.15	6.57	7.79	9.19	
front-1b	0.00	0.00	0.00	0.00	0.00	0.00	0.90
front-1c	1.24	3.18	7.14	6.32	7.00	5.53	
top-2	5.61	3.63	17.68	16.01	16.70	7.74	0.00

[a] Except for the B3LYP calculation, energies are computed single points at the optimized MP2 6-31++G(d,p) level geometry. Energies have not been corrected for ZPE or BSSE effects.

interaction), suggesting that the MP2/631++G(d,p) method is a better medium-cost choice than the B3LYP method.

Conclusions

Nine stable [C_4C_1im]Cl ion pair structures were located: the chloride has six possible locations, front, top (and thus bottom), butside, methside and back. The top and front conformers are the lowest in energy, and the methside and butside conformers lie ~30 kJ mol^{-1} higher in energy. The back conformer is ~60 kJ mol^{-1} higher in energy. All the conformers except the top-2 are evident in the various crystal structures. However, the top-2 conformer has now been identified as viable by at least three methodologies: ab initio, classical,[18,19,33] and Car−Parrinello MD studies.[32] Moreover, this conformer, although not observed in the solid state, is more stable than the butside, methside, and back conformers, which are observed in the solid state, and is determined to be essentially degenerate with the most stable front conformers. Flat potential energy surfaces indicate that the Cl^- anion can move locally with very little cost in energy.

The chloride anion of each ion pair, except for the top and back conformers, forms at least one strong H-bond to a C^{ring}−H atom. Frequency analysis indicates that a second H-bond can form with the alkyl chain hydrogen atoms in both the butside and methside conformers. However, in the butside ion pairs, facile rotational of the butyl chain can easily break this H-bond. There is evidence that the "medium"-strength secondary H-bonds are significantly weakened beyond 2.50 Å. In solution, each cation may have six associated Cl^- anions, with longer H-bonds due to the presence of the other anions. However, it is also possible that a mixture of the stronger gas-phase-like ion pairs can form and coexist for a period of time before reverting. Because the Cl^- anion primarily associates with only one of the C^{ring}−H, the remaining ring hydrogen atoms exhibit modes similar to the "bare" cation and are computed to lie between 3290 and 3310 cm^{-1} (and expected to relate to peaks ~150 cm^{-1} lower in the experimental spectrum). Individual conformers will generate additional peaks in the vibrational spectrum. The front ion pairs will contribute a very intense red-shifted C^2−H mode at ~2655 cm^{-1}. Two medium intensity modes will occur between 2960 and 3010 cm^{-1}, one of which will appear as a single slightly split peak (due to the H-bonding in the methside ion pair), while the other may appear as two distinct peaks (due to H-bonding in the butside ion pair). Moreover, the top conformer will contribute two low-intensity red-shifted peaks around 650 and 750 cm^{-1} and a low-intensity blue-shifted peak.

The butyl chain of the $[C_4C_1im]^+$ cation can rotate over a large range of angles for little cost in energy. Three local minima were identified: front-1a (τ_1, τ_2) = (−102°, 180°), front-1b (−83°, −65°), and front-1c (−107°, 64°), where (τ_1, τ_2), τ_1 = C^2−N^1−C^7−C^8 and τ_2 = N^1−C^7−C^8−C^9. The most stable position for the butyl chain changes on association with the Cl^- anion, and τ_1 is altered significantly. The thermodynamically more stable polymorph (orthorhombic)[31] has an imidazolium cation which can be related to the gas-phase front-1b (and front-1c) conformers of [C_4C_1im]Cl, while the less stable polymorph (monoclinic)[13,31] has an imidazolium cation which can be related to the gas-phase front-1a conformer.

Barriers on the potential energy surface for τ_1 are steric and arise from repulsion between hydrogen atoms at C^2 or C^5 on the imidazolium ring and those at C^8 on butyl chain. Barriers for τ_2 relate to steric repulsion between the imidazolium ring and the end group of the butyl chain. The position of C^{butyl}−H close to and directly above N^1 for some conformers is found to be a side effect of other, more dominant, steric interactions; no evidence was found for a significant C_{alkyl}−H···π interaction. The Cl^- anion in the front-1a conformer reduces the steric barrier associated with C^2−H, but slightly increases the more substantial barrier associated with C^5−H. Thus, we anticipate the presence of the anion to enhance rotational movement in the alkyl chains (at low torsional angles) while slightly restricting full rotation. The barriers to rotation are very low and thus will still be active at room temperature, hampering formation of a solid. Thus, the number of stable configurations obtained just for the gas-phase ion pairs is significant; each of the lowest-energy front, top, and bottom Cl^- anion positions can be associated with three alkyl chain positions, giving rise to at least nine almost degenerate configurations, and moreover, the energy required to interconvert these is small. A little higher in energy, and associated with the butside and methside Cl^- anion positions, a further six configurations are possible.

In the gas phase, the imidazolium cations and Cl^- anions obtain significant stabilization from association, ~450 kJ mol^{-1}, indicating why the IL [C_4C_1im]Cl has a negligible vapor pressure. This also indicates that a single cation in the liquid phase can obtain significant stabilization from association with a single Cl^- anion. For example, in solution, loss of one of the six surrounding anions could be temporarily adapted for by forming a stronger H-bond with another of the local anions. Movement of the anions around a cation is relatively facile because of the flat potential energy surfaces in the region of the local minima, and thus, the movement required to "tighten" a single H-bond should not be energetically expensive. Hence, movement of the ions in an IL is facilitated, and a liquid phase is favored. The long hydrogen bonds in [C_4C_1im]Cl indicate that the Cl^- anion is inhibited from approaching the cation too closely; this repulsive effect may also help prevent confinement in a solid array.

Various low-level methods were examined for their ability to predict Cl^- anion association and the potential energy surfaces for butyl chain rotation; our conclusions are that HF/3-21G, HF/3-21+G(d), and B3LYP/3-21G* are all unsuitable. Computations at the HF/6-31G(d) level followed by single-point calculations at the MP2/6-31++G(d,p) level offer a viable low-cost alternative. The relative energy ordering of the rotational local minima varied with the basis set sophistication and the amount of correlation recovered. Energy differences between the rotational conformers were, however, <10 kJ mol^{-1}.

The relative energy of the front and top isomers was discussed with reference to classical MD simulations,[18,19,33] Car−Parrinello MD computations,[32] liquid-phase neutron diffraction studies,[16,17] and related crystal structures.[13,31] The stability of the front versus top conformers of $[C_4C_1im]Cl$ cannot be easily resolved, and it is clear that the energy ordering of these conformers is highly sensitive to the method of computation. Molecular dynamics simulation (both classical (liquid) and Car−Parrinello (gas phase) tend to favor the top conformer.[32] This is in contrast to experimental studies (liquid) and quantum chemical ab initio (gas phase) which tend to favor both. At the highest level of computation attempted here (CCSD(T)/aug-cc-pVDZ)), and in contrast to our gas-phase B3LYP results and recent Car−Parrinello MD results, the two conformers (front and top) are found to be essentially degenerate.[32] Overall, the B3LYP functional combined with a 6-31++G(d,p) basis sets is adequate for determining gross energy differences, but it is incapable of recovering the correct energy ordering for structures that differ subtly because of tensional motion or dispersion effects. Thus, because of active dispersion effects, the MP2/6-31++G(d,p) method is a better choice than DFT methods. However, independent of the computational tool applied, it is clear that the front and top conformers are energetically similar and data from all sources point toward an anion that is highly mobile within the vicinity of the C^2−H bond.

Acknowledgment. P.H. gratefully acknowledges The Royal Society for a University Research Fellowship.

Note Added in Proof. While this paper was under reivew, two papers appeared in which the results of ab initio MD simulations on $[C_1C_1im]Cl$ were reported: Bühl, M.; Chaumont, A.; Schurhammer, R.; Wipff, G. *J. Phys. Chem. B* **2005**, *109*, 18591. Bhargava, B.; Balasubramanian, S. *Chem. Phys. Lett.* **2005**, *417*, 486. A paper by Y. Wang, H. Li, and S. Han (*J. Chem. Phys.* **2005**, *123*, 174501) has also appeared. Using information from this work, we have subsequently located two new structures with the Cl^- anion located in front and to the butyl side of the C^2−H bond where the butyl chain lies in the "a" and "c" positions, with relative energies of 0.61 and 1.38 kJ mol^{-1}, respectively, at the B3LYP/6-31++G(d,p) level and 6.25 and 1.63 kJ mol^{-1}, respectively, at the MP2/6-31++G(d,p) level. The conformer with the butyl chain in the "b" position (as noted in the main text) is unstable and converges to the front-1b structure, which is the lowest energy structure determined by us (so far).

Supporting Information Available: Cartesian coordinates of B3LYP/6-31++G(d,p) optimized ion pairs of $[C_4C_1im]Cl$. B3LYP/6-31++G(d,p) vibrational frequencies of cations and ion pairs. Graph comparing the rotation about τ_1 at the HF/3-21+G(d) and B3LYP/6-31++G(d,p) levels. Table of formation energies, zero point energies, and basis set superposition errors. Figure showing $[C_1C_1im]Cl$ structures front-6 and top-7. This material is available free of charge via the Internet at http://pubs.acs.org.

References and Notes

(1) Welton, T.; Wasserscheid, P. *Ionic Liquids in Synthesis*; VCH-Wiley: Weinheim, 2002.
(2) Dupont, J.; de Souza, R. F.; Saurez, P. A. *Chem. Rev.* **2002**, *102*, 3667.
(3) Chiappe, C.; Pieraccini, D. *J. Phys. Org. Chem.* **2005**, *18*, 275.
(4) Holbrey, J. D.; Seddon, K. R. *Clean Prod. Proc.* **1999**, *1*, 223.
(5) Welton, T. *Coord. Chem. Rev.* **2004**, *248*, 2459.
(6) Wasserscheid, P.; Wilhelm, K. *Angew. Chem., Int. Ed.* **2000**, *39*, 3772.
(7) Wilkes, J. S. *J. Mol. Catal., A* **2004**, *214*, 11.
(8) Del Popolo, M. G.; Voth, G. A. *J. Phys. Chem. B* **2004**, *108*, 1744.
(9) Elaiwi, A.; Hitchcock, P. B.; Seddon, K. R.; Srinivasan, N.; Tan, Y.; Welton, T.; Zora, J. A. *J. Chem. Soc., Dalton Trans.* **1995**, 3467.
(10) Wilkes, J. S.; Zaworotko, M. J. *J. Chem. Soc., Chem. Commun.* **1992**, 965.
(11) Kölle, P.; Dronskowski, R. *Inorg. Chem.* **2004**, *43*, 2803.
(12) Dupont, J.; Saurez, P. A.; De Souza, R. F.; Burrow, R. A.; Kintzinger, J. *Chem.−Eur. J.* **2000**, *6*, 2377.
(13) Saha, S.; Hayashi, S.; Kobayashi, A.; Hamaguchi, H. *Chem. Lett.* **2003**, *32*, 740.
(14) Mele, A.; Tran, C. D.; De Paoli Lacerda, S. H. *Angew. Chem., Int. Ed.* **2003**, *36*, 4364.
(15) Hitchcock, P. B.; Seddon, K. R.; Welton, T. *J. Chem. Soc., Dalton Trans.* **1993**, *17*, 2639.
(16) Hardacre, C.; Holbrey, J. D.; McMath, S. E.; Bowron, D. T.; Soper, A. K. *J. Chem. Phys.* **2003**, *118*, 273.
(17) Hardacre, C.; McMath, S. E.; Nieuwenhuyzen, M.; Bowron, D. T.; Soper, A. K. *J. Phys.: Condens. Matter* **2003**, *15*, S159.
(18) Hanke, C. G.; Price, S. L.; Lynden-Bell, R. M. *Mol. Phys.* **2001**, *99*, 801.
(19) Urahata, S.; Ribeiro, M. *J. Chem. Phys.* **2004**, *120*, 1855.
(20) Fuller, J.; Carlin, R. T.; De Long, H. C.; Haworth, D. *J. Chem. Soc., Chem. Commun.* **1994**, 299.
(21) Noda, A.; Hayamizu, K.; Watanabe, M. *J. Phys. Chem. B* **2001**, 4603.
(22) Hayamizu, K.; Aihara, Y.; Nakagawa, H.; Nukuda, T.; Price, W. S. *J. Phys. Chem. B.* **2004**, *108*, 19527.
(23) de Andrade, J.; Böes, E. S.; Stassen, H. *J. Phys. Chem. B* **2002**, *106*, 13344.
(24) Margulis, C. J. *Mol. Phys.* **2004**, *102*, 829.
(25) Yan, T.; Burnham, C. J.; Del Popolo, M. G.; Voth, G. A. *J. Phys. Chem. B* **2004**, *108*, 2004.
(26) Kobrak, M. N.; Znamenskiy, V. *Chem. Phys. Lett.* **2004**, *395*, 127.
(27) Alavi, S.; Thompson, D. L. *J. Chem. Phys.* **2005**, *122*, 154704.
(28) Every, H.; Bishop, A. G.; Forsyth, M.; MacFarlane, D. R. *Electrochim. Acta* **2000**, *45*, 1279.
(29) Consorti, C. S.; Suarez, P. A.; De Souza, R. F.; Burrow, R. A.; Farrar, D. H.; Lough, A. J.; Loh, W.; da Silva, L. H.; Dupont, J. *J. Phys. Chem. B* **2005**, *10*, 4341.
(30) Gozzo, F. C.; Santos, L. S.; Augusti, R.; Consorti, C. S.; Dupont, J.; Eberlin, M. N. *Chem.−Eur. J.* **2004**, *10*, 6187.
(31) Holbrey, J. D.; Reichert, W. M.; Nieuwenhuyzen, M.; Johnston, S.; Seddon, K. R.; Rogers, R. D. *Chem. Commun.* **2003**, 1636.
(32) Del Popolo, M. G.; Lynden-Bell, R. M.; Kohanoff, J. *J. Phys. Chem. B* **2005**, *109*, 5895.
(33) Liu, Z.; Haung, S.; Wang, W. *J. Phys. Chem. B* **2004**, *108*, 12978.
(34) Bühl, M.; Chaumont, A.; Schurhammer, R.; Wipff, G. *J. Phys. Chem. B* **2005**, *109*, 18591.
(35) Shah, J. K.; Brennecke, J. F.; Maginn, E. J. *Green Chem.* **2002**, *4*, 112.
(36) de Andrade, J.; Böes, E. S.; Stassen, H. *J. Phys. Chem. B* **2002**, *106*, 3546.
(37) Morrow, T. I.; Maginn, E. J. *J. Phys. Chem. B* **2002**, *106*, 12807.
(38) Margulis, C. J.; Stern, H. A.; Berne, B. J. *J. Phys. Chem. B* **2002**, *106*, 12017.
(39) Lynden-Bell, R. M. *Mol. Phys.* **2003**, *101*, 2625.
(40) Cadena, C.; Anthony, J. L.; Shah, J. K.; Morrow, T. I.; Brennecke, J. F.; Maginn, E. J. *J. Am. Chem. Soc.* **2004**, *126*, 5300.
(41) Lopes, J.; Deschamps, J.; Padua, A. *J. Chem. Phys. B* **2004**, *108*, 2038.
(42) Case, D. A.; Pearlman, D. A.; Caldwell, J. W.; III, T. E. C.; Ross, W. S.; Simmerling, C. L.; Darden, T. A.; Merz, K. M.; Stanton, R. V.; Cheng, A. L.; Vincent, J. J.; Crowley, M.; Tsui, V.; Gohlke, H.; Radmer, R. J.; Duan, Y.; Pitera, J.; Massova, I.; Seibel, G. L.; Singh, U. C.; Weiner, P. K.; Kollman, P. A. AMBER; University of California, San Francisco, 2002.
(43) Chaumont, A.; Engler, E.; Wipff, G. *Inorg. Chem.* **2003**, *42*, 5348.
(44) Chaumont, A.; Schurhammer, R.; Wipff, G. *J. Phys. Chem. B* **2005**, *109*, 18964.
(45) Chaumont, A.; Wipff, G. *Phys. Chem. Chem. Phys.* **2003**, *5*, 3481.
(46) Chaumont, A.; Wipff, G. *Inorg. Chem.* **2004**, *43*, 5891.
(47) Chaumont, A.; Wipff, G. *J. Phys. Chem. B* **2004**, *108*, 3311.
(48) Chaumont, A.; Wipff, G. *Chem.−Eur. J.* **2004**, *10*, 3919.
(49) Chaumont, A.; Wipff, G. *Phys. Chem. Chem. Phys.* **2005**, *7*, 1926.
(50) Takahashi, S.; Suzuya, K.; Kohara, S.; Koura, N.; Curtiss, L. A.; Saboungi, M. *Z. Phys. Chem.* **1999**, *209*, 209.
(51) Meng, Z.; Dölle, A.; Carper, W. R. *THEOCHEM* **2002**, *585*, 119.
(52) Talaty, E. R.; Raja, S.; Storhaug, V. J.; Dölle, A.; Carper, W. R. *J. Phys. Chem. B* **2004**, *108*, 13177.

(53) Paulechka, Y. U.; Kabo, G. J.; Blokhin, A. V.; Vydrov, A. O.; Magee, J. W.; Frenkel, M. *J. Chem. Eng. Data* **2003**, *48*, 457.
(54) Carper, W. R.; Mains, G. J.; Piersma, B. J.; Mansfield, S. W.; Larive, C. K. *J. Phys. Chem.* **1996**, *100*, 4724.
(55) Mains, G. J.; Nantsis, E. A.; Carper, W. R. *J. Phys. Chem. A* **2001**, *105*, 4371.
(56) Takahashi, S.; Curtiss, L. A.; Gosztola, D.; Koura, N.; Saboungi, M. *Inorg. Chem.* **1995**, *34*, 2990.
(57) Shah, J. K.; Maginn, E. J. *Fluid Phase Equlib*. **2004**, *222*−*223*, 195.
(58) Turner, E. A.; Pye, C. C.; Singer, R. D. *J. Phys. Chem. A* **2003**, *107*, 2277.
(59) Binkley, J. S.; Pople, J. A.; Hehre, W. J. *J. Am. Chem. Soc.* **1980**, *102*, 939.
(60) Gordon, M. S.; Binkley, J. S.; Pople, J. A.; Pietro, W. J.; Hehre, W. J. *J. Am. Chem. Soc.* **1982**, *104*, 2797.
(61) Pietro, W. J.; Francl, M. M.; Hehre, W. J.; Defrees, D. J.; Pople, J. A.; Binkley, J. S. *J. Am. Chem. Soc.* **1982**, *104*, 5039.
(62) Francl, M. M.; Pietro, W. J.; Hehre, W. J.; Binkley, J. S.; DeFrees, D. J.; Pople, J. A.; Gordon, M. S. *J. Chem. Phys.* **1982**, *77*, 3654.
(63) Hariharan, P. C.; Pople, J. A. *Theo. Chim. Acta* **1973**, *28*, 213.
(64) Clark, T.; Chandrasekhar, J.; Spitznagel, G. W.; Schleyer, P. v. R. *J. Comput. Chem.* **1983**, *4*, 294.
(65) Frisch, M. J.; Trucks, G. W.; Schlegel, H. B.; Scuseria, G. E.; Robb, M. A.; Cheeseman, J. R.; Montgomery, J. A., Jr.; Vreven, T.; Kudin, K. N.; Burant, J. C.; Millam, J. M.; Iyengar, S. S.; Tomasi, J.; Barone, V.; Mennucci, B.; Cossi, M.; Scalmani, G.; Rega, N.; Petersson, G. A.; Nakatsuji, H.; Hada, M.; Ehara, M.; Toyota, K.; Fukuda, R.; Hasegawa, J.; Ishida, M.; Nakajima, T.; Honda, Y.; Kitao, O.; Nakai, H.; Klene, M.; Li, X.; Knox, J. E.; Hratchian, H. P.; Cross, J. B.; Bakken, V.; Adamo, C.; Jaramillo, J.; Gomperts, R.; Stratmann, R. E.; Yazyev, O.; Austin, A. J.; Cammi, R.; Pomelli, C.; Ochterski, J. W.; Ayala, P. Y.; Morokuma, K.; Voth, G. A.; Salvador, P.; Dannenberg, J. J.; Zakrzewski, V. G.; Dapprich, S.; Daniels, A. D.; Strain, M. C.; Farkas, O.; Malick, D. K.; Rabuck, A. D.; Raghavachari, K.; Foresman, J. B.; Ortiz, J. V.; Cui, Q.; Baboul, A. G.; Clifford, S.; Cioslowski, J.; Stefanov, B. B.; Liu, G.; Liashenko, A.; Piskorz, P.; Komaromi, I.; Martin, R. L.; Fox, D. J.; Keith, T.; Al-Laham, M. A.; Peng, C. Y.; Nanayakkara, A.; Challacombe, M.; Gill, P. M. W.; Johnson, B.; Chen, W.; Wong, M. W.; Gonzalez, C.; Pople, J. A. *Gaussian 03*; Gaussian, Inc.: Wallingford, CT, 2004.
(66) Becke, A. D. *J. Chem. Phys.* **1993**, *98*, 5648.
(67) Lee, C.; Yang, W.; Parr, R. G. *Phys. Rev. B* **1988**, *37*, 785.
(68) Perdew, J. P.; Burke, K.; Ernzerhof, M. *Phys. Rev. Lett.* **1996**, *77*, 3865.
(69) Meijer, E. J.; Sprik, M. *J. Chem. Phys.* **1996**, *105*, 8684.
(70) Woon, D. E.; Dunning, T. H. *J. Chem. Phys.* **1993**, 1358.
(71) Dunning, T. H. *J. Chem. Phys.* **1989**, *90*, 1007.
(72) Karlström, G.; Lindh, R.; Malmqvist, P.-Å.; Roos, B. O.; Ryde, U.; Veryazov, V.; Widmark, P.-O.; Cossi, M.; Schimmelpfennig, B.; Neogrady, P.; Seijo, L. *Comput. Mater. Sci.* **2003**, *28*, 222.
(73) Avent, A. G.; Chaloner, P. A.; Day, M. P.; Seddon, K. R.; Welton, T. *J. Chem. Soc., Dalton Trans.* **1994**, 3405.
(74) Suarez, P. A.; Einloft, S.; Dullius, J. L.; De Souza, R. F.; Dupont, J. *J. Chim. Phys. Phys.*−*Chim. Bio.* **1998**, *95*, 1626.
(75) Jeffrey, G. A. *THEOCHEM* **1998**, *485*−*486*, 293.
(76) Taylor, R.; Kennard, O. *J. Am. Chem. Soc.* **1982**, *104*, 5063.
(77) Bondi, A. *J. Phys. Chem.* **1964**, *98*, 441.
(78) Meot-Ner, M. *Chem. Rev.* **2005**, *105*, 213.
(79) Hayashi, S.; Ozawa, R.; Hamaguchi, H. *Chem. Lett.* **2003**, *32*, 498.
(80) Cammarata, L.; Kazarian, S. G.; Salter, P. A.; Welton, T. *Phys. Chem. Chem. Phys.* **2001**, *3*, 5192.
(81) Arduengo, A. J.; Dias, H. V.; Harlow, R. L.; Kline, M. *J. Am. Chem. Soc.* **1992**, *114*, 5530.
(82) Jensen, F. *Introduction to Computational Chemistry*; John Wiley & Sons: Chichester, 1999.
(83) Rauhut, G.; Pulay, P. *J. Phys. Chem.* **1995**, *99*, 3093.
(84) Dieter, K. M.; Dymek, C. J. J.; Heimer, N. E.; Rovang, J. W.; Wilkes, J. S. *J. Am. Chem. Soc.* **1988**, *110*, 2722.